Separation Science and Technology
Publication details, including instructions for authors and subscription information:
http://www.informaworld.com/smpp/title~content=t713708471

Transport of Binary Mixtures in Pervaporation through a Microporous Silica Membrane: Shortcomings of Fickian Models

Ben Bettens[a]; Jan Degrève[a]; Bart Van der Bruggen[a]; Carlo Vandecasteele[a]
[a] Department of Chemical Engineering, K.U. Leuven, Leuven, Belgium

To cite this Article Bettens, Ben , Degrève, Jan , Van der Bruggen, Bart and Vandecasteele, Carlo(2007) 'Transport of Binary Mixtures in Pervaporation through a Microporous Silica Membrane: Shortcomings of Fickian Models', Separation Science and Technology, 42: 1, 1 — 23
To link to this Article: DOI: 10.1080/01496390600998102
URL: http://dx.doi.org/10.1080/01496390600998102

Separation Science and Technology, 42: 1–23, 2007

ISSN 0149-6395 print/1520-5754 online
DOI: 10.1080/01496390600998102

Transport of Binary Mixtures in Pervaporation through a Microporous Silica Membrane: Shortcomings of Fickian Models

Ben Bettens, Jan Degrève, Bart Van der Bruggen, and Carlo Vandecasteele
Department of Chemical Engineering, K.U. Leuven, Leuven, Belgium

Abstract: This study explores the applicability of the adsorption-diffusion mechanism to describe the transport of binary "methanol-water" and "ethanol-water" mixtures in pervaporation through a commercial microporous silica membrane. Two different adsorption-diffusion models are considered: one based on Fick's diffusion equation and another based on the Maxwell-Stefan formulation. Basic models (Fick) assume concentration independent parameters; more complex models (Maxwell-Stefan) incorporate flux coupling and other non-idealities.

The influence of feed temperature (40°C–90°C) on permeation flux was analysed in terms of activation energy for flux, permeability and diffusion, and heat of adsorption and vaporization. Also the occurrence of coupling effects was studied by determining the effect of feed composition (entire composition range) on permeation flux, permeability and selectivity.

Adsorption-diffusion models based on Fick's diffusion equation can be used to describe coupling effects if they are modified with concentration dependent diffusion and/or sorption coefficients. They are incapable of describing drag effects by water on alcohols. These drag effects should be modeled through models based on the Maxwell-Stefan theory.

Keywords: Adsorption-diffusion, Fick, Maxwell-Stefan, microporous silica, pervaporation

Received 6 June 2006, Accepted 29 August 2006
Address correspondence to Ben Bettens, Department of Chemical Engineering, K.U. Leuven, W. de Croylaan 46, B-3001 Leuven, Belgium. Tel.: +32 16 32 23 44; Fax: +32 16 32 29 91; E-mail: ben.bettens@cit.kuleuven.be

INTRODUCTION

One of the main application areas of pervaporation in the industry today, is the dewatering of organic liquids using nonporous hydrophilic membranes. Pervaporative dehydration of these short-chain alcohols, glycols, carboxylic acids, esters, ethers, ketones, amines, nitriles, and halogenated hydrocarbons is important since most of these—forming azeotropes which cannot easily be separated by distillation—are commonly used solvents in many chemical syntheses. Therefore, their recovery is an economical and environmental necessity (1–4).

Most hydrophilic membranes commercially available are made of polyvinyl alcohol (PVA), crosslinked by special agents to reduce excessive swelling. Research emphasis is on the development of new polymeric membranes exhibiting a better stability under various operating conditions (2). Attention is also increasingly being paid to the development of inorganic microporous membranes such as ceramics and zeolites, which are more resistant to harsh chemical, thermal and pressure conditions (5). The successful implementation of these membranes in industrial processes requires a high membrane selectivity and permeability.

Apart from the optimization of the membrane material and the membrane design itself, it is important to know how the membrane performs under varying process conditions. Consequently, reliable data on selectivity and permeability need to be gathered over wide ranges of composition, temperature, and pressure. These data can then be used to develop an accurate model of the mass transfer through the selective layer in pervaporation.

Over the years the theoretical modeling of multi-component mass transport across nonporous membranes has been taken to various levels of detail. Firstly, the applicability of a model depends on the membrane class: polymeric membranes or inorganic membranes (6, 7). Secondly, the focus should not be exclusively on mass transfer through the selective layer of the membrane but also on additional influences on the overall mass transfer related to resistances in the support layer(s) (3, 8) and in the bulk phase (concentration polarization (9)). Thirdly, a good model should consider phenomena such as permeate pressure drop (3), heat transfer (temperature drop (10)) and membrane fouling (9). Fourthly, a model that holds information on non-steady-state performance of the pervaporation membrane is indispensable during the start-up of the pervaporation process and in bioconversion processes and chemical reactions where feed composition changes (11). Fifthly, a model should incorporate equilibrium (sorption) and kinetic (diffusion) coupling of components in a multi-component mixture (12). Finally, the applicability of a model depends on the concentration interval considered. For example, Sommer et al. (13) reported that the water flux was linearly dependent on the water content in the feed when they examined water–methanol pervaporation with water contents between 0.1 and 20 wt%. However, it is generally believed that in many cases, this kind of linear relationship can only be expected at very low water feed concentrations.

In a previous paper (14), it was found that the steady-state permeation mechanism of pure components through a microporous silica membrane obeys the adsorption-diffusion description. This paper studies the transport behavior of binary mixtures methanol-water and ethanol-water through a similar membrane. The steady-state experimental fluxes are correlated with the feed temperature (40–90°C) and the feed composition (0–90 wt% water) to verify whether an activated process still dominates, or whether deviations occur in which permeability also depends on the other feed component and its concentration (coupling effects). The experimental results are discussed in terms of Fick's diffusion equation (15, 16) and the Maxwell-Stefan theory (15–18). Since the microporous silica membrane is water selective, water depletion in the boundary layer can occur at low water concentrations in the feed; especially at high permeate fluxes. However, with increasing flow velocity, concentration polarization is decreased. In this work a high flow velocity is applied, corresponding to a turbulent regime (Re = 12000). Hence, it is assumed that the mass transfer resistances in bulk phase and temperature drop over the membrane are negligible.

THEORY

This work is based on the adsorption-diffusion theory for ceramic membranes (17–20). The membrane is considered to be nonporous so that transport occurs only by diffusion and not by convection. Transport of a component from the feed solution through the membrane occurs by

1. sorption onto the membrane,
2. diffusion through the membrane and
3. desorption from the membrane (usually not explicitly considered since mostly very fast).

Mass transfer resistances in bulk phase and temperature drop over the membrane are neglected since the flow is turbulent (Re = 12000). Transport in the membrane top layer is assumed to be the rate-controlling step (21).

Based on the adsorption-diffusion theory, a number of pervaporation models have been developed, expressing the performance of the membrane in terms of the flux and separation factor. In this work two types of models are considered:

1. models derived from Fick's binary diffusion equation (15, 16) and
2. models derived from the Maxwell-Stefan theory (15–18).

The mathematical equations behind both types of models are given for a binary mixture being transported through a membrane.

Adsorption-Diffusion Models based on Fick's Diffusion Equation

Fick's law of binary diffusion postulates a linear dependence of the diffusion flux of species i, with respect to the average mixture velocity, and its composition gradient. If c_1 and c_2 are the molar concentrations of component 1 and 2 and c is the total mixture molar concentration, then the diffusion flux J_1 is usually related to the molar fraction gradient (∇x) by (15, 16)

$$J_1 = -cD_{12}\nabla x_1 \tag{1}$$

where D_{12} is the binary Fick diffusivity. An analogous relation can be written for component 2.

Equation (1) may be integrated over the membrane to give (for a constantly assumed diffusion coefficient D_{12}):

$$J_1 = \frac{D_{12}}{L}\left(c_{m1}^{\text{feed}} - c_{m1}^{\text{perm}}\right) \tag{2}$$

where L is the membrane thickness and c_{m1}^{feed}, c_{m1}^{perm} are the concentrations inside the membrane on the feed side and on the permeate side, respectively.

Under the assumption that, in pervaporation through a microporous silica membrane, the components are transported as vapor species via surface diffusion, the vapor concentration in the membrane at the membrane interface may be obtained through Henry's law that makes use of the solubility parameter, S. It is defined by the expression (18)

$$c_{m1} = S_{m1} \cdot P_1 \tag{3}$$

where P_1 is the partial pressure of component 1 in the phase adjoining the interface. The linear relationship (3) only holds at low levels of adsorption.

The Fickian approach in combination with Henry's law leads to the following solution-diffusion equation (17–20).

$$J_1 = S_{m1} \cdot D_{m1} \cdot \frac{P_1^{\text{feed}} - P_1^{\text{perm}}}{L} = F_{m1} \cdot \frac{\Delta P_1}{L} \tag{4}$$

In this equation $\Delta P_1 = P_1^{\text{feed}} - P_1^{\text{perm}}$ represents the partial pressure difference over the membrane and $F_{\text{m1}} = S_{\text{m1}}\, D_{\text{m1}}$ is termed the permeability.

The separation performance of a membrane is expressed in terms of the separation factor, which is a combination of the membrane selectivity and the selectivity resulting from the vapor-liquid equilibrium at the membrane interface. The separation factor α is usually defined as (22)

$$\alpha_{12} = \frac{y_1/y_2}{x_1/x_2} \tag{5}$$

where x and y are the molar fractions of components in the retentate and permeate, respectively.

The ideal separation factor (for ideal mixtures) is defined as the ratio of the pure component permeabilities (22).

$$\alpha_{12}^{ID} = \frac{F_{m1}}{F_{m2}} \tag{6}$$

The temperature dependence of the flux follows an Arrhenius (exponential) type of relation, with E_J the activation energy for flux (23).

$$J = J_0 \exp\left(-\frac{E_J}{RT}\right) \tag{7}$$

Since the driving force ΔP_i is also temperature dependent via the Clausius-Clapeyron equation, it is more convenient to compare membrane systems based on the activation energy for permeability E_F, which is a combination of the activation energy for diffusion (E_D) and the heat of adsorption (ΔH_s). The difference in activation energy for flux and permeability is the heat of vaporization ΔH^{vap} (23):

$$E_F = E_D - \Delta H_S \tag{8}$$

$$E_F = E_J - \Delta H^{\text{vap}} \tag{9}$$

In general, solubility and Fickian diffusivity are concentration dependent. The permeating components do not only interact with the membrane but also with each other. This may result in the diffusivity of a component in a mixture being higher than the diffusivity of the same pure component (due to kinetic or flux coupling). Exponential or linear forms often express the concentration dependence of diffusivity. These interactions may also result in deviations from Henry's law so other sorption models (e.g., Langmuir or Freundlich) are required (equilibrium coupling). Different empirical expressions of concentration dependence of solubility and/or diffusivity have been incorporated into (4). However, its applicability is limited to the experimentally established range in variables for which empirical parameters were derived (12, 15, 16).

Adsorption-Diffusion Models based on the Maxwell-Stefan Theory

In case two or more components are present inside a membrane, the system is actually at least ternary (multi-component) in nature, so the ordinary binary diffusion equation (Fick) does not always work correctly. Therefore, the transport of a binary mixture of components 1 and 2 permeating through the membrane is better described by the Maxwell-Stefan equations as a ternary mixture of components 1, 2, and M (membrane). The transport equation for component 1 is based on the driving force of component 1, and the friction

of this component with the membrane and with component 2. Under the assumption that the components are transported as individual vapor species (15–18)

$$-\frac{1}{P_1}\frac{dP_1}{dz} = \frac{x_2}{Đ_{12}}\left(\frac{J_1}{c_1} - \frac{J_2}{c_2}\right) + \frac{1}{Đ'_{1M}}\frac{J_1}{c_1} \tag{10}$$

where z is the coordinate perpendicular to the membrane surface, $Đ_{12}$ the Maxwell-Stefan diffusivity between components 1 and 2, $Đ'_{1M}$ the Maxwell-Stefan diffusivity of component 1 in the membrane and x_2 the average molar fraction of component 2 in the adsorbed phase.

If $J_2/c_2 \ll J_1/c_1$ (for example in dehydration applications; 1 = water and 2 = solute) and assuming Henry's law (3) applies, explicit expressions for J_1 and J_2 can be obtained from (10) (17, 18)

$$J_1 = S_{m1}\left(\frac{Đ_{12}Đ'_{1M}}{Đ'_{1M}x_2 + Đ_{12}}\right)\frac{\Delta P_1}{L} \tag{11}$$

$$J_2 = S_{m2}Đ'_{2M}\frac{\Delta P_2}{L} + \frac{x_2Đ'_{2M}}{Đ_{12}}J_1 \tag{12}$$

EXPERIMENTAL

A tubular microporous silica membrane, supplied by Pervatech (Enter, The Netherlands) was studied. The ceramic tube had an inner diameter of 7 mm and an outer diameter of 10 mm and consisted of an α-alumina support, a γ-alumina intermediate layer and a silica top layer coated on the inner surface of the hollow fiber. The effective membrane length and the effective membrane area were 23 cm and 50.58 cm^2, respectively. The mean pore size and the thickness of the silica layer were 0.3–0.55 nm and 10–20 nm, respectively (24).

All pervaporation experiments were carried out with the laboratory test cell described in Van Baelen et al. (25) (lab test cell unit, Sulzer Chemtech, Neunkirchen, Germany). Permeate was collected in glass traps cooled in liquid nitrogen in a Dewar flask. Vacuum was maintained using a two-stage vacuum pump. Permeate was collected by switching between two glass traps in parallel, so that the connection between the permeate side and the vacuum pump was never closed. Using this procedure, the permeate pressure was always below 10 mbar.

Experiments were performed with methanol-water and ethanol-water mixtures over the full concentration range. According to recommendations from the manufacturers, the membrane was not used with pure water, due to possible stability problems. The temperature was varied between 40°C and 90°C. The feed flow rate was 250 l/h, resulting in a Reynolds number of approximately 12000 (turbulent flow).

Methanol and ethanol were both technical grade and were obtained from Merck (Amsterdam, The Netherlands). The permeate alcohol composition was determined with a Shimadzu GC-14A gas chromatograph.

The partial feed pressure of the permeating component was calculated using: $P_i^{\text{feed}} = P_i^{\text{vap}} \gamma_i x_i$, where x_i is the molar fraction of component i in the liquid phase, γ_i the activity coefficient at temperature T(K) and P_i^{vap} the vapor pressure of pure i at temperature T(K). The values of γ_i were calculated with the UNIQUAC equation (26), and P_i^{vap} with the Clausius-Clapeyron equation. The partial permeate pressure was calculated using: $P_i^{\text{perm}} = y_i P^{\text{perm}}$, with y_i the permeate molar fraction and P^{perm} the total pressure (27).

RESULTS AND DISCUSSION

Effect of Temperature on Flux and Selectivity

Figure 1 shows the total mass flux for the different methanol-water mixtures as a function of temperature. The total flux J shows an Arrhenius-like dependence on temperature, indicating that the pervaporative transport is an activated process. The partial methanol flux and the partial water flux also increase with increasing temperature (not shown). The flux trend for the ethanol-water system (not shown) is similar to that of the methanol-water system.

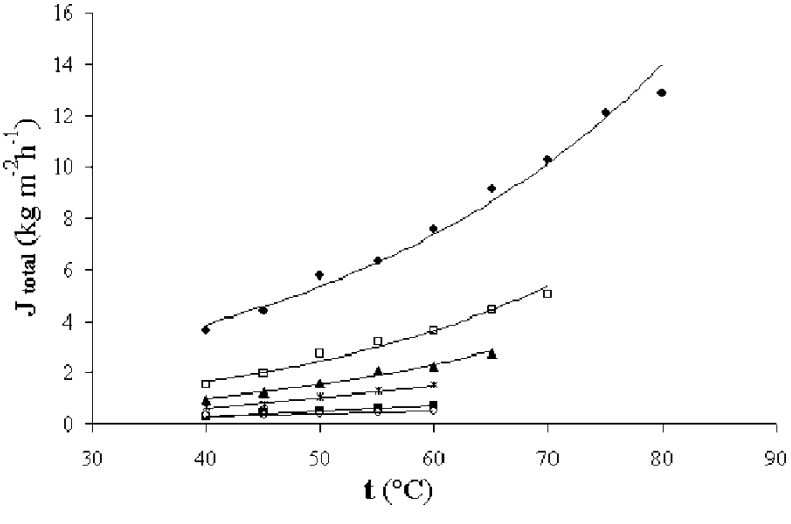

Figure 1. Total mass flux (J) of water-methanol mixtures as a function of temperature (t); (●) = 10 vol% MetOH, (□) = 30 vol% MetOH, (▲) = 50 vol% MetOH, (∗) = 70 vol% MetOH, (■) = 90 vol% MetOH, (○) = 100% MetOH.

Since the partial water and partial alcohol flux both increase with increasing temperature, there is only a minor temperature effect on selectivity. For low alcohol contents in the mixtures, the separation factor remains almost constant at every temperature or decreases slightly. For higher alcohol contents the separation factor increases because the water flux increases more on increasing temperature than the partial alcohol flux does. This is shown for the ethanol-water system in Fig. 2 and can be explained by the constant size of the pores: while the number of molecules transported across the membrane increases with higher temperature given a large driving force, the relative distribution of the various molecules remains fairly unaffected (28). The separation factor trend for the methanol-water system (not shown) is similar.

The activation energies for flux and permeability are found from the slopes (-E/R) of the straight-line correlations between the logarithm of flux and permeability, respectively, versus the inverse of absolute temperature values (14). Quantitative data extracted from the experimental results are listed in Table 1. Numerical values of activation energies for flux E_J are in the range of 8–52 kJ/mol and are comparable to those found by ten Elshof et al. (18) and Sommer et al. (13). Furthermore, these values overlap with the range of the heat of vaporization for water, methanol and ethanol (28–64 kJ/mol in temperature interval 20–95°C) (29), so that negative values of activation energies for permeability E_F occur. This indicates that the membrane permeability decreases with increasing temperature, which implies a heat of adsorption larger than the respective activation energy for

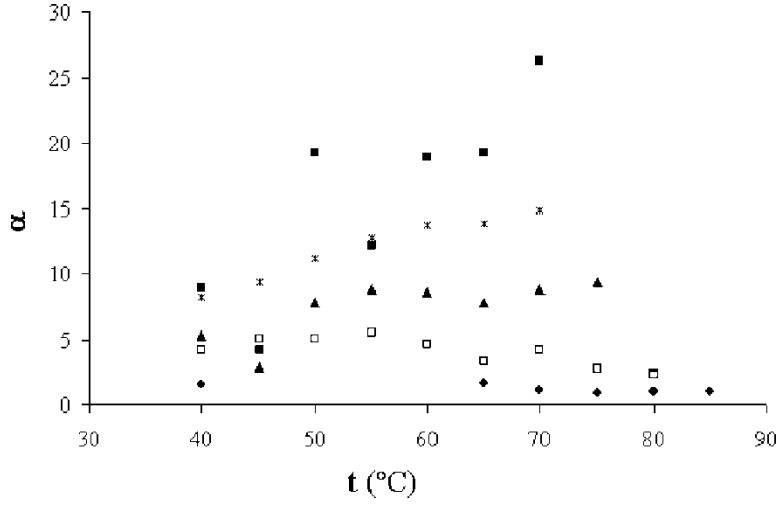

Figure 2. Separation factor (α) of water-ethanol mixtures as a function of temperature (t); (●) = 10 vol% EtOH, (□) = 30 vol% EtOH, (▲) = 50 vol % EtOH, (∗) = 70 vol% EtOH, (■) = 90 vol% EtOH.

Table 1. Activation energies for flux and permeability for water, methanol and ethanol (kJ/mol) as a function of feed concentration (vol%)

Vol% MetOH	E_J (kJ/mol)		E_F (kJ/mol)		Vol% EtOH	E_J (kJ/mol)		E_F (kJ/mol)	
	MetOH	Water	MetOH	Water		EtOH	Water	EtOH	Water
100	21.9		−16.1		100	16.2		−25.8	
90	22.4	41.1	−15.1	−7.1	90	15.0	51.5	−26.9	4.0
70	20.8	43.7	−17.1	−2.8	70	22.4	37.4	−19.5	−7.6
50	8.94	2.2	−29.0	−7.7	50	29.2	47.7	−7.5	2.8
30	17.6	34.4	−19.8	−9.7	30	46.1	31.1	4.7	−13.7
10	30.8	29.2	−7	−15.8	10	31.7	16.5	−9.0	−30.7
Avg.	20	38	− 17	− 9	Avg.	27	37	− 14	− 9

diffusion (30). Finally, the average activation energies for methanol and ethanol are comparable and lower than for water, again confirming that on average, selectivity slightly increases with increasing temperature.

Effect of Composition on Flux and Selectivity: Results

The pure component permeate fluxes (symbol (○) in Fig. 1) are listed in Table 2. At 60°C the flux is 0.499 kg/m^{2}h for methanol and 0.185 kg/m^{2}h for ethanol. This higher flux for methanol is mainly attributed to a higher dielectric constant (31) and Hansen parameter (32) (polarity parameters) and to a lesser extent to a smaller molecular weight (29) or kinetic diameter (30) (size parameters). Sommer et al. (22) measured a pure methanol flux of 0.12 kg/m^2 h for a similar Pervatech membrane at 60°C and a pure ethanol flux of 0.06 kg/m^{2}h at 70°C.

For mixtures, the total and partial alcohol fluxes are listed in Tables 3 and 4 as a function of concentration and temperature. Sommer et al. (22) measured 0.39 kg/m^2 h (methanol-water, 10.5 wt% water, 60°C) and

Table 2. Pure alcohol flux as a function of temperature

t (°C)	Pure methanol flux (kg/m^{2}h)	Pure ethanol flux (kg/m^{2}h)
40	0.31	0.12
45	0.33	0.14
50	0.41	0.18
55	0.45	0.17
60	0.50	0.19
65		0.18
70		0.23

Table 3. Binary total alcohol-water fluxes as a function of concentration (vol%) and temperature

Flux (kg/m^2h) t (°C)	M/W 10–90	E/W 10–90	M/W 30–70	E/W 30–70	M/W 50–50	E/W 50–50	M/W 70–30	E/W 70–30	M/W 90–10	E/W 90–10
40	3.7	9.8	1.5	3.0	0.97	0.87	0.65	0.70	0.29	0.42
45	4.4	—	1.9	3.8	1.3	1.1	0.80	0.91	0.45	0.48
50	5.8	—	2.8	4.3	1.6	1.7	1.0	1.1	0.50	0.60
55	6.3	—	3.2	5.8	2.1	2.2	1.3	1.6	0.64	0.74
60	7.6	—	3.6	7.2	2.2	2.6	1.5	1.7	0.73	1.0
65	9.1	14	4.4	8.2	2.7	2.8		1.9		1.2
70	10	13	5.0	9.4		4.1		2.3		1.4
75	12	17		11		5.0				
80	13	18		12						
85		28								

M/W = Methanol-water, E/W = Ethanol-water.

Table 4. Binary partial alcohol fluxes as a function of concentration (vol %) and temperature

Flux (kg/m^2h) t (°C)	M/W 10–90	E/W 10–90	M/W 30–70	E/W 30–70	M/W 50–50	E/W 50–50	M/W 70–30	E/W 70–30	M/W 90–10	E/W 90–10
40	0.037	0.72	—	0.26	0.23	0.13	0.23	0.15	0.14	0.22
45	0.037	—	0.081	0.28	0.17	0.24	0.27	0.16	0.29	0.21
50	0.045	—	0.11	0.31	0.18	0.18	0.35	0.19	0.36	0.20
55	0.061	—	0.11	0.41	0.18	0.22	0.35	0.24	0.37	0.23
60	0.063	—	0.12	0.52	0.18	0.26	0.37	0.25	0.43	0.26
65	0.084	0.89	0.13	0.90	0.21	0.29		0.27		0.34
70	0.097	1.1	0.15	0.94		0.40		0.30		0.32
75	0.11	2.0		1.2		0.51				
80	0.13	2.4		1.8						
85		3.7								

M/W = Methanol-water, E/W = Ethanol-water.

2.00 kg/m^2 h (ethanol-water, 11.0 wt %, 70°C), which is of the same order of magnitude as the values in Table 3.

In contrast to the results of the pure component permeate fluxes, the total fluxes for the methanol-water system are a little below those of the ethanol-water system (Table 3) as a result of the lower partial water flux for the methanol-water system. This effect is in part attributed to the lower activity of water in the mixture, as methanol is more polar than ethanol (33). A plot of the activity as a function of the water weight percentage at 40°C is given in Fig. 3 (26). However, the lower activity of water in the methanol-water mixtures alone cannot explain the large differences in partial water flux between methanol-water and ethanol-water systems at high water concentration. Also the lower permeability of water in methanol-water mixtures at high water concentration is a factor to consider (Table 5). Sorption experiments will be performed to further examine the reasons for this different water permeability with different alcohols. Except at low water concentrations, the partial water flux is higher than the partial alcohol flux (by a factor of 10). This highlights the hydrophilic character of the microporous silica membrane.

Figure 4 shows the total mass flux for the different methanol-water mixtures as a function of feed composition. Ethanol-water mixtures exhibit similar trends (not shown). For both alcohol-water systems, the total flux and the partial water flux (not shown) increase with increasing water content. In the region of technical interest (low water content) the increase is almost proportional with the water content. At high water contents, linearity does not hold.

The partial alcohol flux decreases with increasing water content in the case of methanol and increases in the case of ethanol. This is shown in

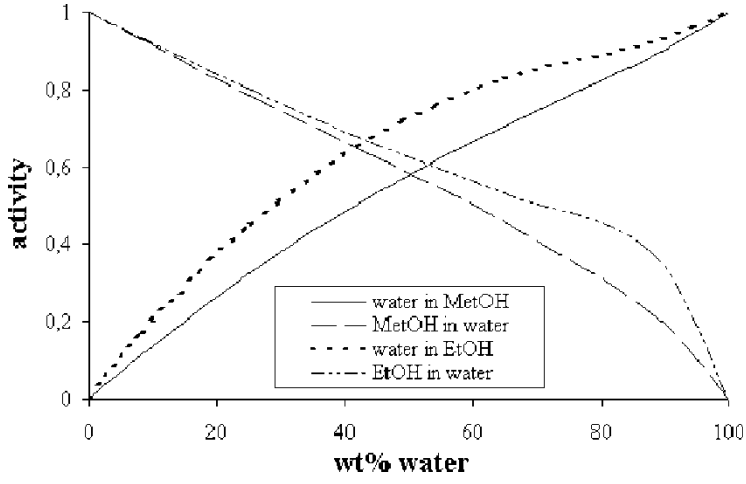

Figure 3. Activity as a function of the water weight percentage at 40°C (26).

Table 5. Permeability of water as a function of concentration (vol%) and temperature

Permeability (kg/m^2h bar)	M/W	E/W	M/W	E/W	M/W	E/W	M/W	E/W	M/W	E/W
t (°C)	10–90	10–90	30–70	30–70	50–50	50–50	70–30	70–30	90–10	90–10
40	61	169	—	46	16	13	12	11	7.4	6.5
45	57	—	26	45	18	11	12	11	5.4	5.9
50	55	—	28	39	17	15	12	11	5.2	7.4
55	47	—	26	41	18	15	12	12	5.4	6.7
60	44	—	23	40	16	14	12	10	4.6	7.7
65	42	58	22	34	15	12		9.0		6.9
70	37	43	21	32		14		8.6		7.1
75	35	43		28		14				
80	30	37		25						
85		46								

M/W = Methanol-water, E/W = Ethanol-water.

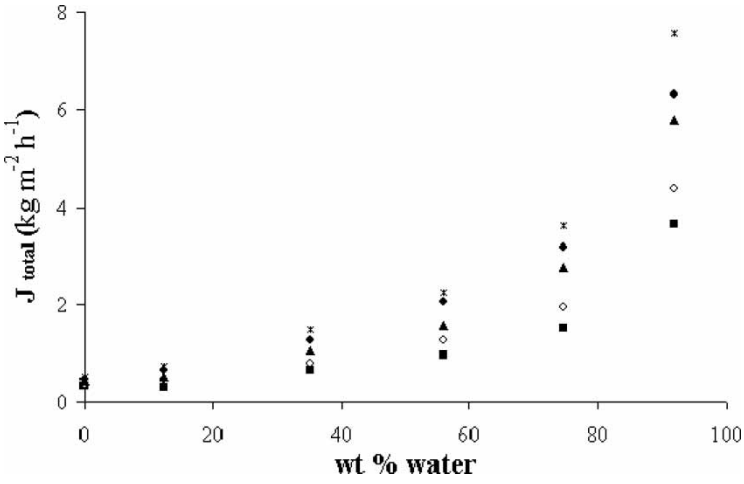

Figure 4. Total mass flux (J) of water-methanol mixtures as a function of water content (wt%) in the feed; (■) = 40°C, (○) = 45°C, (▲) = 50°C, (●) = 55°C, (∗) = 60°C.

Figs. 5a and 5b, respectively. The latter is often attributed to the so-called drag effect due to the simultaneous flux of water (22). As a result the separation factor increases with increasing water content for the water-methanol system (on average from $\alpha = 5$ at 10 wt% water to $\alpha = 15$ at 90 wt% water) and decreases for the water-ethanol system (on average from $\alpha = 13$ at 10 wt% water to $\alpha = 2$ at 90 wt% water). This is shown in Figs. 6a and 6b, respectively. An alternative representation, similar to the yx-equilibrium diagram used in distillation, is the plot (Fig. 7) of the permeate concentration versus the feed concentration, complemented by the reference line illustrating the relevant vapor-liquid equilibrium (34).

Effect of Composition on Flux and Selectivity: Evaluation of Adsorption-Diffusion Models

With respect to the applicability of an adsorption-diffusion model to describe transport through a microporous silica membrane, the following conclusions can be drawn from Figs. 3 to 7:

1. Deviations from the ideal solution-diffusion model may be caused by interactions between the different components in the feed. The occurrence of these interactions can be seen in Fig. 3 "activity versus wt% water," and is also known to exist from the vapor liquid equilibrium diagram in Fig. 7 (ethanol-water even shows an azeotrope).
2. Since the membrane was not used with pure water according to recommendations from the manufacturers, the ideal separation factor, defined in (6) as

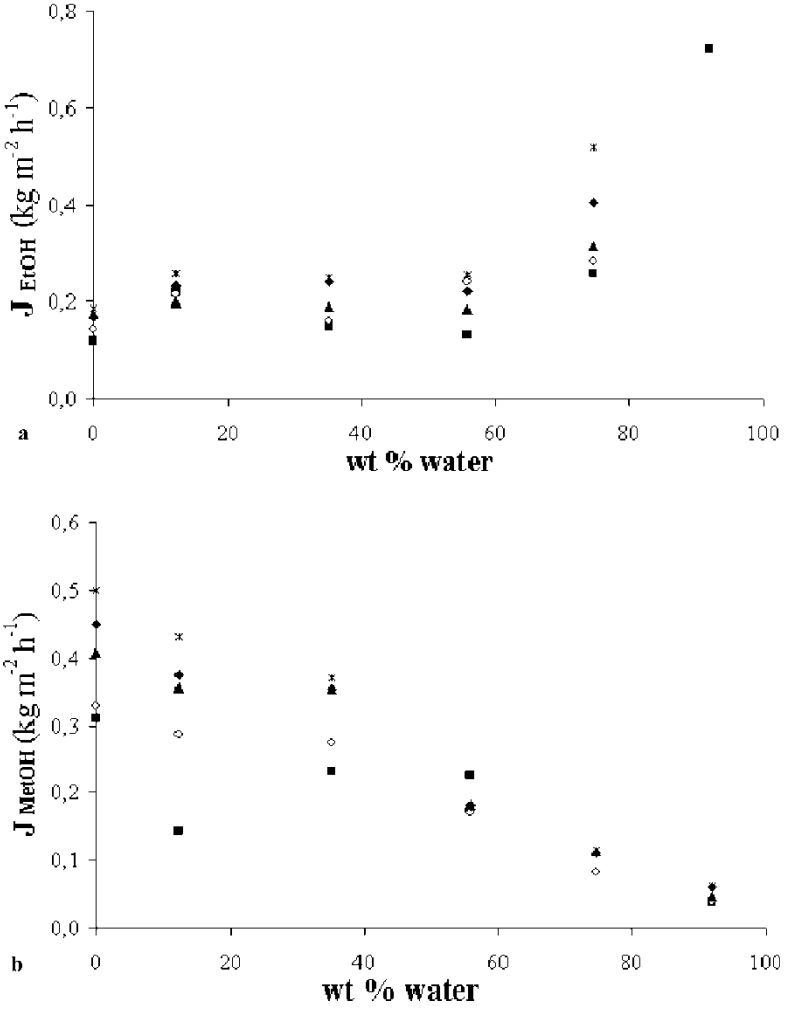

Figure 5. Partial alcohol flux (J) of (a) water-methanol and (b) water-ethanol mixtures as a function of water content (wt%) in the feed; (■) = 40°C, (○) = 45°C, (▲) = 50°C, (●) = 55°C, (∗) = 60°C.

the ratio of the pure component permeabilities, cannot be determined. However, when the water permeabilities of the 90% water mixtures are used, its value should exceed 70 for methanol-water and 190 for ethanol-water. From Fig. 6 it is clear that ideal and mixture separation factors differ a lot. Moreover, the mixture separation factors depend on concentration. This also suggests that competing adsorption and/or diffusion effects play a major role in the pervaporation of binary mixtures.

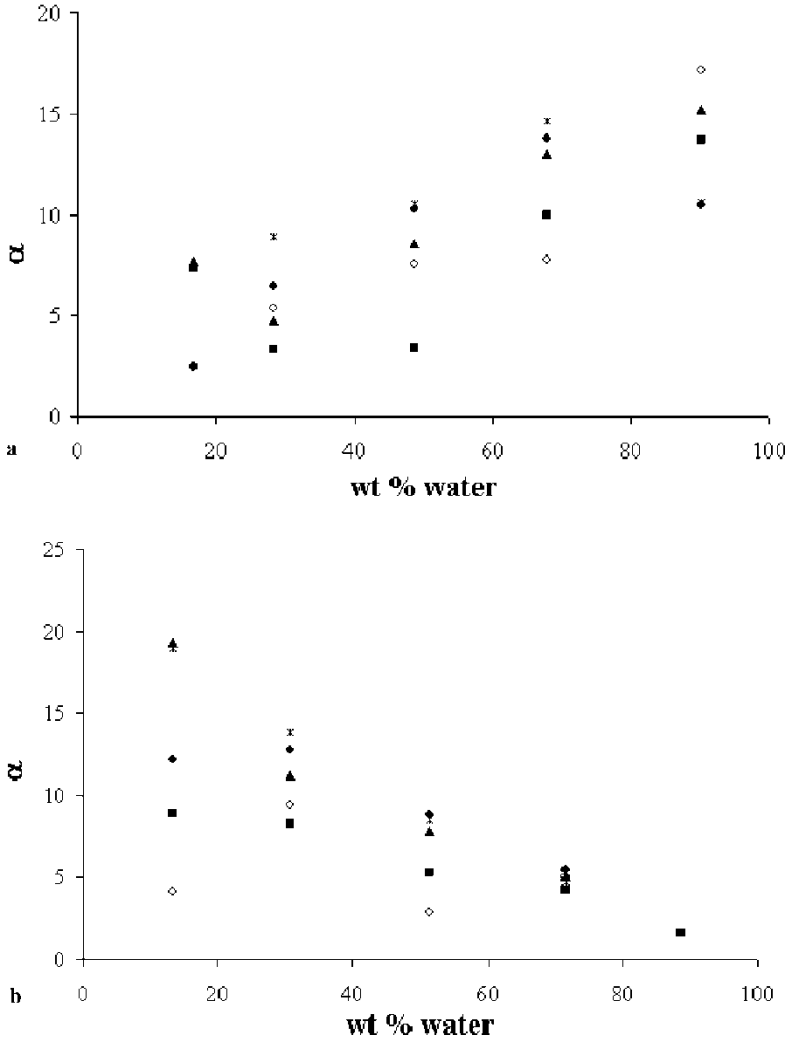

Figure 6. Separation factor (α) of (a) water-methanol and (b) water-ethanol mixtures as a function of water content (wt%) in the feed; (■) = 40°C, (○) = 45°C, (▲) = 50°C, (●) = 55°C, (∗) = 60°C.

3. The nonlinear behavior of the total mass flux as a function of feed concentration in Fig. 4 suggests a concentration dependent permeability. To verify this, the driving force (the partial pressure difference over the membrane) is used instead of the feed concentration. This is done for water, methanol and ethanol in Figs. 8a, 8b and 8c respectively.

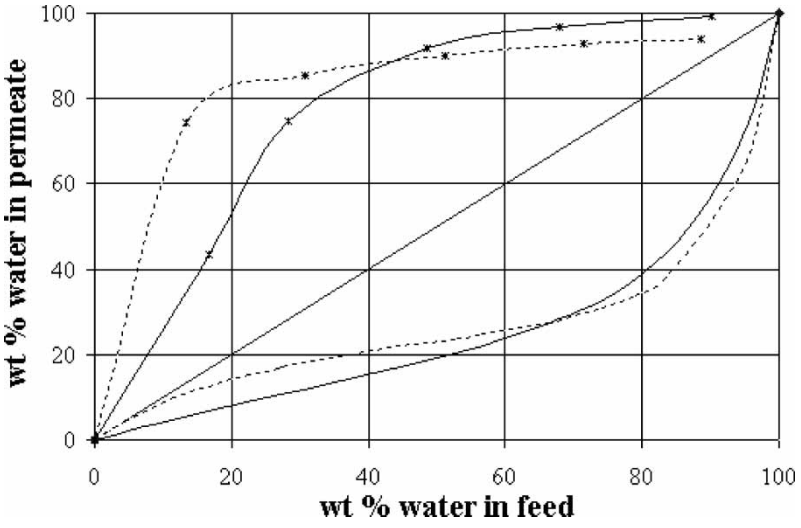

Figure 7. Permeate water content (wt%) as a function of water content (wt%) in the feed at 60°C for methanol-water (∗ and full line) and ethanol-water (∗ and broken line) and vapor-liquid equilibrium for methanol (full line) and ethanol (broken line).

At low water content, when there is an excess of alcohol in the feed, there is an increased competition for sorption sites, resulting in lower water permeation. This is shown in Fig. 8a. Increasing the water concentration and hence the driving force for water transport, increases the partial water permeability (found as the slope of the curve and given in Table 5) (25). In future research sorption experiments will be conducted to elucidate the mechanism of competitive sorption.

Besides competitive sorption, the interaction between water and alcohol can also be regarded as the result of the concentration dependence via x_2 of the diffusion term $Đ_{12}\ Đ'_{1M}/(Đ'_{1M}\ x_2 + Đ_{12})$ in equation (11). Since $J_2/c_2 \ll J_1/c_1$, (11) applies with $1 =$ water, $2 =$ alcohol. Information on diffusion coefficients can also be obtained from sorption experiments (35).

Figure 8b shows that the partial methanol flux is only dependent on the driving force for methanol and is independent of changes in the water concentration. Assuming the mass transport in the membrane top layer to be the rate-controlling step (21), the mass flux according to (4) is given by:

$$J_{MetOH} = \frac{S_{MetOH} \cdot D_{MetOH}}{L} \Delta P_{MetOH} = 0.61 \cdot \Delta P_{MetOH} \qquad (13)$$

Verkerk et al. (17) estimated the adsorption coefficient for methanol to be approximately 0.6 $\mathrm{mol/m^3 \cdot Pa}$ (1920 $\mathrm{kg/m^3 \cdot bar}$) at 60°C. Ten Elshof et al. (18) used a value of 3.8 $\mathrm{mol/m^3 \cdot Pa}$ (12160 $\mathrm{kg/m^3 \cdot bar}$) at 60°C. The thickness of the membrane used in this study is 20 nm. With these values,

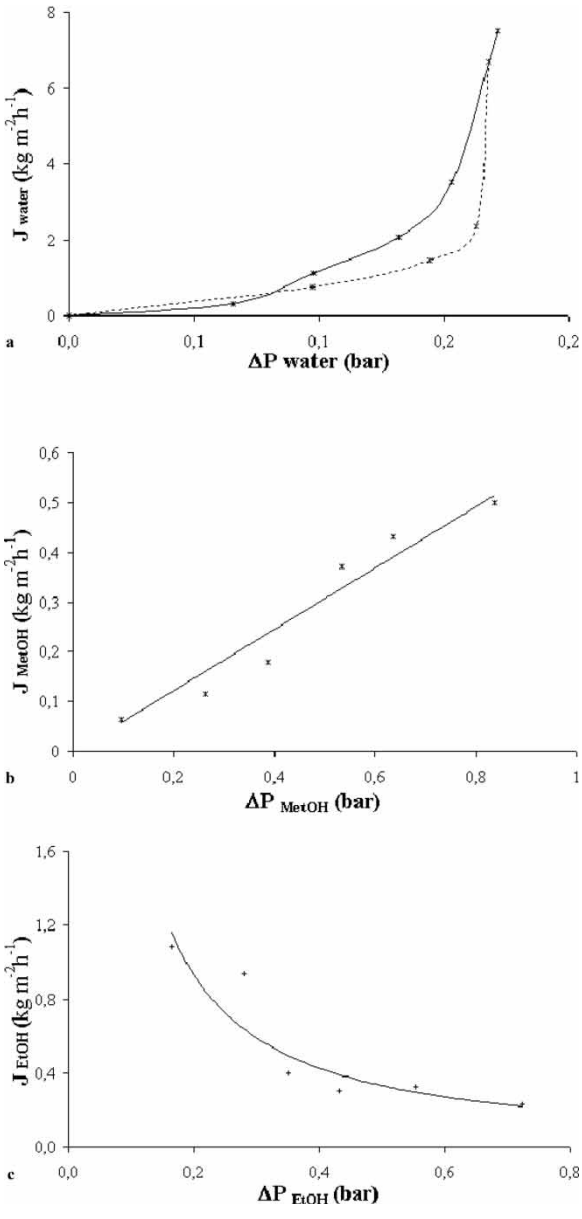

Figure 8. (a) Partial water flux as a function of the driving force for water (partial pressure difference in bar) at 60°C for methanol-water (∗ and full line) and ethanol-water (∗ and broken line). Lines are to guide the eye. (b) Partial methanol flux as a function of the driving force for methanol (partial pressure difference in bar) at 60°C for methanol-water. Linear correlation $r^2 = 0.95$. (c) Partial ethanol flux as a function of the driving force for ethanol (partial pressure difference in bar) at 70°C for ethanol-water. Line is to guide the eye.

a Fick diffusion coefficient D_{MetOH} of $2 \cdot 10^{-15}$ m^2/s or $3 \cdot 10^{-16}$ m^2/s respectively, is calculated. This corresponds to the values obtained by ten Elshof et al. (18).

In terms of the Maxwell-Stefan theory, with $x_2/Đ_{12} \ll 1/Đ'_{1M}$ (1 = MetOH, 2 = water), (11) becomes:

$$J_{MetOH} = \frac{S_{MetOH} Đ'_{MetOH}}{L} \Delta P_{MetOH} \tag{14}$$

For this case the Fick and Maxwell-Stefan diffusivity are identical to each other ($D = Đ'$) (16).

Figure 8c shows a decreasing partial ethanol flux with increasing driving force for ethanol. Ethanol is not polar enough to be significantly sorbed into the membrane, in contrast to methanol. However, if water is sufficiently present, permeation of ethanol is possible, presumably because the ethanol molecules can be shielded from the membrane by water molecules surrounding the ethanol (25). This is often attributed to the so-called drag effect (22) due to the simultaneous flux of water and alcohol. This drag-effect cannot be modeled through the binary Fick equation since a negative permeability is non-physical. However, to explain the experimentally observed trend in the ethanol flux in terms of the Maxwell-Stefan theory, it has to be assumed that the term containing the partial water flux dominates the term containing the ethanol flux.

CONCLUSIONS

The Arrhenius temperature dependence of the steady-state fluxes in methanol-water and ethanol-water systems through a microporous silica membrane indicates that the transport of these binary mixtures is an activated process that obeys the adsorption-diffusion description. The heats of adsorption for water and alcohol are larger than the respective activation energies for diffusion; hence permeability decreases with increasing temperature. Selectivity on the other hand, slightly increases with increasing temperature.

From the effect of concentration on flux, permeability and selectivity, it is obvious that pronounced coupling effects determine the mass transfer of mixtures through the membrane. Where the methanol flux is relatively independent on water activity, the partial water flux is influenced by even a small amount of alcohol through preferential adsorption or diffusion coupling. Ethanol molecules can also be dragged across the membrane with the permeating water.

Adsorption-diffusion models based on Fick's diffusion equation can be used to describe some coupling effects if they are modified with concentration dependent diffusion and/or sorption coefficients. However they are incapable of describing a drag effect by water on alcohols. This drag effect can be modeled in a better way through models based on the Maxwell-Stefan theory. Here also, information on the concentration dependence of diffusion

and sorption is needed. Future research will focus on competitive sorption and diffusion of mixtures as a function of concentration.

NOMENCLATURE

c	Concentration (mol m^{-3})
D	Binary Fick diffusion coefficient (m^2 h^{-1})
$Đ$	Maxwell-Stefan diffusion coefficient (m^2 h^{-1})
E_D	Activation energy for diffusion (J mol^{-1})
E_F	Activation energy for permeability (J mol^{-1})
E_J	Activation energy for flux (J mol^{-1})
F	Permeability coefficient (mol m^{-1} h^{-1} bar^{-1} or kg m^{-1} h^{-1} bar^{-1})
J	Flux (mol m^{-2} h^{-1} or kg m^{-2} h^{-1})
L	Membrane thickness (m)
P	Partial vapor pressure (bar)
P^{perm}	Total permeate pressure (bar)
P^{vap}	Vapor pressure (bar)
R	Gas constant (8,3143 J mol^{-1} K^{-1})
S	Adsorption coefficient or solubility (mol m^{-3} bar^{-1} or kg m^{-3} bar^{-1})
t	Temperature (°C)
T	Temperature (K)
x	Mole fraction (−)
x	Average molar fraction in Equation (10)
x	Feed molar fraction (−)
y	Permeate molar fraction (−)
z	Coordinate perpendicular to the membrane surface

Greek Letters

α	Separation factor
γ	Activity coefficient (−)
ΔH_s	Heat of adsorption (J mol^{-1})
ΔH^{vap}	Heat of vaporization (J mol^{-1})
ΔP	Transmembrane partial pressure difference (bar)

Subscripts

0	Reference temperature
i	Component i
feed	Feed

m	Membrane
perm	Permeate

Superscript

ID	Ideal

ACKNOWLEDGMENT

The Research Council of the K.U. Leuven is gratefully acknowledged for financial support (OT/2002/33). Pervatech is thanked for kindly supplying membrane samples.

REFERENCES

1. Kujawski, W. (2000) Application of pervaporation and vapor permeation in environmental protection. *Polish J. Environ. Stud.*, 9: 13–26.
2. Jonquières, A., Clément, R., Lochon, P., Néel, J., Dresch, M., and Chrétien, B. (2002) Industrial state-of-the-art of pervaporation and vapour permeation in the western countries. *J. Membr. Sci.*, 206: 87–117.
3. de Bruijn, F.T., Sun, L., Olujić, Ž, Jansens, P.J., and Kapteijn, F. (2003) Influence of the support layer on the flux limitation in pervaporation. *J. Membr. Sci.*, 223: 141–156.
4. Sommer, S., Klinkhammer, B., and Melin, T. (2002) Integrated system design for dewatering of solvents with microporous silica membranes. *Desalination*, 149 (1–3): 15–21.
5. van Veen, H.M., van Delft, Y.C., Engelen, C.W.R., and Pex, P.P.A.C. (2001) Dewatering of organics by pervaporation with silica membranes. *Sep. Purif. Technol.*, 22–23: 361–366.
6. Feng, X. and Huang, R.Y.M. (1997) Liquid separation by membrane pervaporation: a review. *Ind. Eng. Chem. Res.*, 36: 1048–1066.
7. Lipnizki, F. and Trägårdh, G. (2001) Modelling of pervaporation: models to analyze and predict the mass transport in pervaporation. *Separ. Purif. Meth.*, 30 (1): 49–125.
8. Trifunović, O. and Trägårdh, G. (2005) The influence of support layer on mass transport of homologous series of alcohols and esters through composite pervaporation membranes. *J. Membr. Sci.*, 259: 122–134.
9. Vane, L.M. and Alvarez, F.R. (2005) Vibrating pervaporation modules: Effect of module design on performance. *J. Membr. Sci.*, 255 (1–2): 213–224.
10. Ito, A., Feng, Y., and Sasaki, H. (1997) Temperature drop of feed liquid during pervaporation. *J. Membr. Sci.*, 133 (1): 95–102.
11. Schäfer, T., Vital, J., and Crespo, J.G. (2004) Coupled pervaporation/mass spectrometry for investigating membrane mass transport phenomena. *J. Membr. Sci.*, 241: 197–205.
12. Ghoreyshi, S.A.A., Farhadpour, F.A., and Soltanieh, M. (2002) Multicomponent transport across nonporous polymeric membranes. *Desalination*, 144: 93–101.

13. Sommer, S. and Melin, T. (2005) Influence of operation parameters on the separation of mixtures by pervaporation and vapor permeation with inorganic membranes. Part 1: Dehydration of solvents. *Chem. Eng. Sci.*, 60 (16): 4509–4523.
14. Bettens, B., Dekeyzer, S., Van der Bruggen, B., Degreve, J., and Vandecasteele, C. (2005) Transport of pure components in pervaporation through a microporous silica membrane. *J. Phys. Chem. B.*, 109 (11): 5216–5222.
15. Bird, R.B., Stewart, W.E., and Lightfoot, E.N. (2002) *Transport Phenomena*, 2nd ed.; Wiley: New York.
16. Taylor, R. and Krishna, R. (1993) *Multicomponent Mass Transfer*; Wiley: New York.
17. Verkerk, A.W., Van Male, P., Vorstman, M.A.G., and Keurentjes, J.T.F. (2001) Description of dehydration performance of amorphous silica pervaporation membranes. *J. Membr. Sci.*, 193: 227–238.
18. ten Elshof, J.E., Abadal, C.R., Sekulić, J., Chowdhury, S.R., and Blank, D.H.A. (2003) Transport mechanisms to water and organic solvents through microporous sillica in the pervaporation of binary liquids. *Micropor. Mesopor. Mat.*, 65: 197–208.
19. Shieh, J.-J. and Huang, R.Y.M. (1998) A pseudophase-change solution diffusion model for pervaporation/Single component permeation. *Separ. Sci. Technol.*, 33 (6): 767–785.
20. Shieh, J.-J. and Huang, R.Y.M. (1998) A pseudophase-change solution diffusion model for pervaporation/Binary mixture permeation. *Separ. Sci. Technol.*, 33 (7): 933–957.
21. Kölsch, P., Sziládi, M., Noack, M., Caro, J., Kotsis, L., Kotsis, I., and Sieber, I. (2002) Ceramic membranes for water separation from organic solvents. *Chem. Eng. Technol.*, 25 (4): 357–362.
22. Sommer, S. and Melin, T. (2005) Performance evaluation of microporous inorganic membranes in the dehydration of industrial solvents. *Chem. Eng. Proc.*, 44 (10): 1138–1156.
23. Feng, X. and Huang, R.Y.M. (1996) Estimation of activation energy for permeation in pervaporation processes. *J. Membr. Sci.*, 118: 127–131.
24. Casado, C., Urtiaga, A., Gorri, D., and Ortiz, I. (2005) Pervaporative dehydration of organic mixtures using a commercial silica membrane – Determination of kinetic parameters. *Separ. Purif. Technol.*, 42 (1): 39–45.
25. Van Baelen, D., Reyniers, A., Van der Bruggen, B., Vandecasteele, C., and Degrève, J. (2004) Pervaporation of binary and ternary mixtures of water with methanol and/or ethanol. *Separ. Sci. Technol.*, 39 (3): 563–580.
26. www.vlecalc.org(accessed Feb. 2002).
27. Wijmans, J.G. and Baker, R.W. (1993) A simple predictive treatment of the permeation process in pervaporation. *J. Membr. Sci.*, 79: 101–113.
28. Gallego-Lizon, T., Ho, Y.S., and dos Santos, L.F. (2002) Comparative study of commercially available polymeric and microporous silica membranes for the dehydration of IPA/water mixtures by pervaporation/vapour permeation. *Desalination*, 149: 3–8.
29. Perry, R.H. and Green, D. (1984) *Perry's Chemical Engineers' Handbook*, 6th ed.; McGraw-Hill International Editions.
30. Bowen, T.C., Li, S., Noble, R.D., and Falconer, J.L. (2003) Driving force for pervaporation through zeolite membranes. *J. Membr. Sci.*, 225: 165–176.
31. Machado, D.R., Hasson, D., and Semiat, R. (1999) Effect of solvent properties on permeate flow through nanofiltration membranes Part I. Investigation of parameters affecting solvent flux. *J. Membr. Sci.*, 163: 93–102.

32. Hansen, C.M. and Smith, A.L. (2004) Using Hansen solubility parameters to correlate solubility of C_{60} fullerene in organic solvents and in polymers. *Carbon*, 42: 1591–1597.
33. Shah, D., Kissick, K., Ghorpade, A., Hannah, R., and Bhattacharyya, D. (2000) Pervaporation of alcohol-water and dimethylformamide-water mixtures using hydrophilic zeolite NaA membranes. *J. Membr. Sci.*, 179 (1–2): 185–205.
34. Noble, R.D. and Stern, S.A. (1995) *Membrane Separations Technology, Principles and Applications*; Elsevier: Amsterdam.
35. Mamaliga, I., Schabel, W., and Kind, M. (2003) Measurement of sorption isotherms and diffusion coefficients by means of a magnetic suspension balance. *Chem. Eng. Proc.*, 43: 753–763.